# REPORT DOCUMENTATION PAGE

Form Approved
OMB No. 0704-0188



| 1. REPORT DATE *(DD-MM-YYYY)* | 2. REPORT TYPE | 3. DATES COVERED *(From - To)* |
|---|---|---|
| | Technical Papers | |

**4. TITLE AND SUBTITLE**

Please see attached

**5a. CONTRACT NUMBER**

**5b. GRANT NUMBER**

**5c. PROGRAM ELEMENT NUMBER**

**6. AUTHOR(S)**

**5d. PROJECT NUMBER**
1011

**5e. TASK NUMBER**
0011

**5f. WORK UNIT NUMBER**
549859

**7. PERFORMING ORGANIZATION NAME(S) AND ADDRESS(ES)**

Air Force Research Laboratory (AFMC)
AFRL/PRS
5 Pollux Drive
Edwards AFB CA 93524-7048

**8. PERFORMING ORGANIZATION REPORT**

**9. SPONSORING / MONITORING AGENCY NAME(S) AND ADDRESS(ES)**

Air Force Research Laboratory (AFMC)
AFRL/PRS
5 Pollux Drive
Edwards AFB CA 93524-7048

**10. SPONSOR/MONITOR'S ACRONYM(S)**

**11. SPONSOR/MONITOR'S NUMBER(S)**
Please see attached

**12. DISTRIBUTION / AVAILABILITY STATEMENT**

Approved for public release; distribution unlimited.

**13. SUPPLEMENTARY NOTES**

**14. ABSTRACT**

20030130 110

**15. SUBJECT TERMS**

| 16. SECURITY CLASSIFICATION OF: | | | 17. LIMITATION OF ABSTRACT | 18. NUMBER OF PAGES | 19a. NAME OF RESPONSIBLE PERSON |
|---|---|---|---|---|---|
| a. REPORT | b. ABSTRACT | c. THIS PAGE | | | Leilani Richardson |
| Unclassified | Unclassified | Unclassified | A | | 19b. TELEPHONE NUMBER *(include area code)* (661) 275-5015 |

11

MEMORANDUM FOR PRS (In-House Publication)

FROM: PROI (STINFO) 02 May 2002

SUBJECT: Authorization for Release of Technical Information, Control Number: **AFRL-PR-ED-TP-2002-093**
Greg Spanjers (PRSS) et al., "Advanced Diagnostics for Millimeter-Scale Micro Pulsed Plasma Thrusters"

**AIAA Plasmadynamics & Lasers Conference** **(Statement A)**
**(20-23 May 2002, Maui, HI) (Deadline: ASAP)**

**1.** This request has been reviewed by the Foreign Disclosure Office for: a.) appropriateness of distribution statement, b.) military/national critical technology, c.) export controls or distribution restrictions, d.) appropriateness for release to a foreign nation, and e.) technical sensitivity and/or economic sensitivity.
Comments:_____

Signature _____ Date _____

2. This request has been reviewed by the Public Affairs Office for: a.) appropriateness for public release and/or b) possible higher headquarters review.
Comments: _____

Signature _____ Date _____

**3.** This request has been reviewed by the STINFO for: a.) changes if approved as amended, b) appropriateness of references, if applicable; and c.) format and completion of meeting clearance form if required
Comments:_____

Signature _____ Date _____

4. This request has been reviewed by PR for: a.) technical accuracy, b.) appropriateness for audience, c.) appropriateness of distribution statement, d.) technical sensitivity and economic sensitivity, e.) military/ national critical technology, and f.) data rights and patentability
Comments:_____

APPROVED/APPROVED AS AMENDED/DISAPPROVED

_____

PHILIP A. KESSEL Date
Technical Advisor
Space and Missile Propulsion Division

# Advanced Diagnostics for Millimeter–Scale Micro Pulsed Plasma Thrusters

Gregory G. Spanjers[‡]
AFRL Propulsion Directorate, Edwards AFB, CA 93524

Erik L. Antonsen[*]
Rodney L. Burton[**]
University of Illinois at Urbana–Champaign, IL 61801

Michael Keidar[§]
Iain D. Boyd[§§]
University of Michigan, Ann Arbor, MI 48109

Stewart S. Bushman
W. E. Research, Rosamond, CA 93560

A class of Micro–Pulsed Plasma Thrusters (MicroPPTs) is being developed by the Air Force Research Laboratory (AFRL) to provide precise attitude control and stationkeeping ability to 25–kg class satellites. Operating by means of a surface discharge across a Teflon™ propellant fuel bar only a few millimeters in diameter, the MicroPPT delivers a thrust–to–power ratio of 5 – 10 μN–s/J. Due to the low pulse energy and size, the MicroPPT produces a spatially–confined and diffuse plasma plume that is difficult to analyze with material probes. Efforts to characterize MicroPPT plume are underway. To this end, a Herriott Cell interferometer is introduced to establish the plume electron and neutral densities. Comparison of the measured electron density with modeling predictions shows close agreement. Additionally, a Pockels cell has been developed to provide a zero–impedance MicroPPT breakdown voltage measurement. Current research focuses on an infrared-emission measurement capability to determine propellant surface temperature during thruster operation.

## Introduction

With the increasing presence of micro–propulsion options for spacecraft attitude control and propulsion, there is a corresponding need for the development of experimental techniques to validate modeling efforts geared towards describing the operating physics of these devices. The Air Force Research Laboratory is currently developing a class of Micro–Pulsed Plasma Thrusters (MicroPPTs) using Teflon™ propellant to provide precise impulse bits in the 10 μN–s range. In the near term, these thrusters can provide propulsive attitude control on 150–kg class spacecraft at 1/10$^{th}$ the dry mass of conventional torque rods and reaction wheels.[1] Eventually, these thrusters are designed for primary and attitude control propulsion on future 25–kg class spacecraft performing missions such as formation flying space–based surveillance and on–orbit satellite servicing. Due primarily to the elimination of the ignitor and corresponding circuit, the MicroPPTs have realized mass reductions from the standard LES 8/9[1,2] PPT of 60–90%, depending on the specific design.

A simple schematic of the MicroPPT is shown in Figure 1.[3] A high voltage energy storage capacitor is connected directly to a coaxial propellant module. The propellant consists of a central conductive rod that serves as the cathode in the discharge. The cathode is surrounded by an annulus of Teflon, which serves as the primary source of propellant. The Teflon propellant is then encased in a conductive tube, which serves as the anode. In the self–triggering configuration shown in Figure 1, the DC–DC converter charges the capacitor to a high voltage. This voltage also appears at the electrodes and across the propellant face. At some point in the charge cycle, the electrode voltage exceeds the surface breakdown voltage of the propellant face, and the discharge self–initiates. Alternatively, an external ignitor plug can be used to trigger the discharge by supplying a small quantity of seed plasma. The surface discharge then ablates a small amount of the solid Teflon material, ionizes it, and accelerates it from the thruster through primarily electromagnetic forces.

---

[‡]Scientist, Air Force Research Laboratory.
*Ph.D. Candidate, Department of Aeronautical and Astronautical Engineering, Urbana, IL 61801.
** Professor, Department of Aeronautical and Astronautical Engineering, Urbana, IL 61801.
[§]Post–Doctoral, Department of Aerospace Engineering, University of Michigan, Ann Arbor MI 48109.
[§§]Professor, Department of Aerospace Engineering, University of Michigan, Ann Arbor MI 48109.

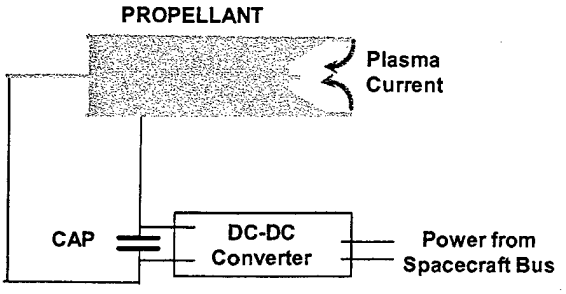


**Figure 1: Simple MicroPPT schematic**

The small plasma volume generated by the MicroPPT creates a significant diagnostic challenge. For material probes, such as electrostatic or magnetic field probes, the characteristic length of the probe is comparable to or larger then the MicroPPT plasma volume.[4] For interferometric techniques to measure density,[5] the measurement resolution is constrained by the short scale length of the plasma. Since the interferometer measures a phase shift proportional to the product of the density and the laser path length through the plasma, the fundamentally short path length results in excessive measurement uncertainty for the line–averaged plasma density.

To address this problem, a Herriott Cell[6] interferometer was used and a technique employing a 'point measurement' was developed.[7] This technique converges multiple laser passes in a Herriott Cell down to a small area, thereby providing increased laser path length within the plasma. By focusing a large number of laser beams into a small measurement volume, the Herriott Cell increases the instrument resolution by a factor of about 10, compared to a single-pass interferometer, with minimal degradation of spatial resolution. Electron density is measured with a single–wavelength Herriott cell and compared with numerical predictions. Efforts to measure the neutral density after the current pulse using a 2nd laser frequency are discussed in a previous work.[8]

Previous modeling efforts have indicated that the plasma distribution in the plume field heavily depends upon upstream boundary conditions.[9,10,11] Therefore the model of the plasma generation in these devices becomes a very important aspect of accurate plasma plume simulation. Inspection of the Micro-PPT propellant surface after firing indicated signs of charring and preferential ablation near the electrodes.[3,12] In this paper we present results of the microscopic analyses of the charred areas and propose a mechanism of the char formation. In order to understand this phenomenon, a model of the

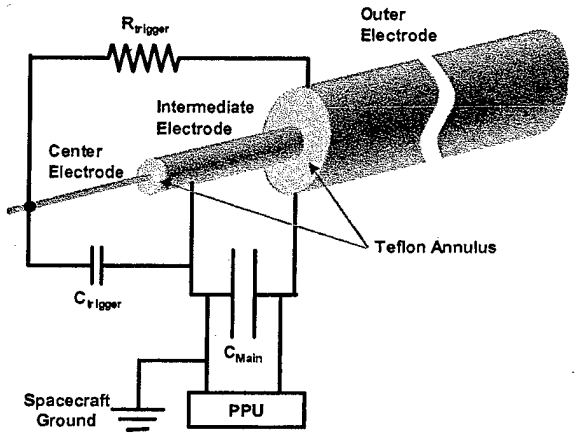


**Figure 2: MicroPPT 3 electrode configuration.**

plasma layer near the Teflon™ surface is developed. In addition, the solution of the model provides boundary conditions for simulating the plasma plume.[13]

## Experimental Apparatus

The vacuum chamber at AFRL used for the Herriott Cell measurements is well–suited for optical diagnostic access to low power electric thrusters. The chamber is 2.1 $m^3$, and base pressures of ~30 μTorr are typical. Optical access is available through several 14–inch viewports.

### *AFRL Micro–PPT Testbed*

The AFRL MicroPPT currently in development for TechSat21 uses a 3 electrode configuration[14], illustrated in Figure 2. A small diameter rod (center electrode) is encased in a small-diameter annulus of Teflon, which is then encased in a relatively small diameter tube which acts as the intermediate electrode. This construction is then encased in a second larger diameter annulus of Teflon, which is then encased in a large diameter outer electrode. The MicroPPT is fired by a low-energy breakdown between the intermediate and central electrode. This discharge provides enough seed ionization to enable the higher energy conduction breakdown between the intermediate and outer electrode. The discharge between the intermediate and central electrode is referred to as the "trigger discharge." The discharge between the intermediate and outer electrode is referred to as the "main discharge."

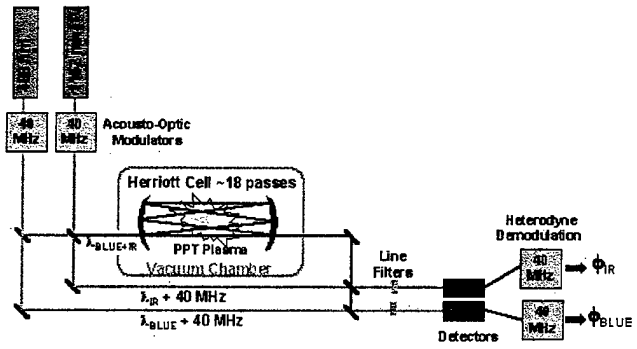


**Figure 3: Interferometer Layout**

Although a wide range of parameters are tested in various MicroPPT configurations, typically the trigger discharge will consume about 1/50 the energy of main discharge. In this fashion, the MicroPPT has demonstrated the ability to passively initiate a surface breakdown discharge across outer propellant diameters as high as 1/4" using a relatively low voltage below 3000V. Without the 3-electrode configuration, up to 40 kV would be required to initiate the discharge across a 1/4" diameter. This would place excessive design requirements on the power-processing unit and on the spacecraft EMI shielding.

In this work, research is performed on simple 2-electrode MicroPPT test-bed configurations. Understanding the physical processes in this geometry has proven beneficial in advancing the optimization of the MicroPPT by separating the requirements for the trigger and main discharges. Research on small diameter 2-electrode designs, generally between 1-3 mm, is applicable to the trigger discharge. Research on larger diameter 2-electrode designs, typically between 3 and 7 mm, are more applicable to the main discharge.

The MicroPPT testbed uses a coaxial geometry with bare copper outer anode and central cathode that is silver–coated copper. The outer diameter of the thrusters tested here is 6.35 mm while the outer Teflon™ diameter is 5.46 mm. The cathode diameter is 1.64 mm. A DC–DC converter charges a 0.417 μF capacitor to 5.6 kV, corresponding to a stored energy of 6.6 J. Not shown in Figure 1 is the external sparkplug used to initiate the discharge in the testbed configuration. A 0.5" diameter plug is placed approximately 2 cm from the propellant face, at a 45-degree angle, and discharged with a 0.5 J capacitor that is triggered from the data acquisition system.

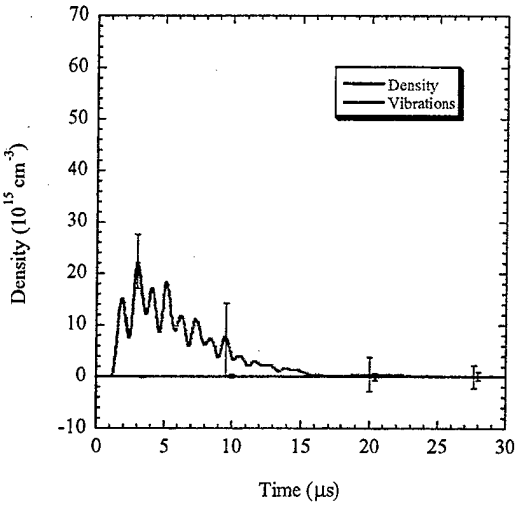


**Figure 4: Electron density with vibrations for 13-pass Herriott Cell. 5 mm from fuel face and 6.6 J.**

*Interferometer Layout*

The interferometer employs quadrature heterodyning technique and a Herriott Cell for increased path length exposure. Detailed descriptions of these are given elsewhere. [8,15,16] Figure 3 gives a general layout of the interferometer with the optional second laser frequency.

A Bragg cell splits the 150 mW Argon–ion laser (488 nm) into scene and reference beams using a 40 MHz shift in the reference beam. The scene beam is directed into the vacuum tank through a viewport and into the Herriott Cell optics. The Herriott Cell optics for the point measurement configuration require the Herriott Cell mirrors as well as focusing and guiding optics for the input and exit beams. The MicroPPT is situated halfway between the Herriott Cell mirrors.

The scene beam is returned to the external optics table and recombined with the reference beam that travels the same path length. The combined beams are focused on the detector for optimal measurement intensity.

*Two–Color Interferometer*

A two–color interferometer was also constructed for baseline comparison of electron and neutral densities. This interferometer allows separation of electron and neutral densities throughout the pulse. A 488–nm Ar–ion laser was used simultaneously with an 1152–nm HeNe laser providing direct measurements of both electron and neutral densities early in the pulse. This

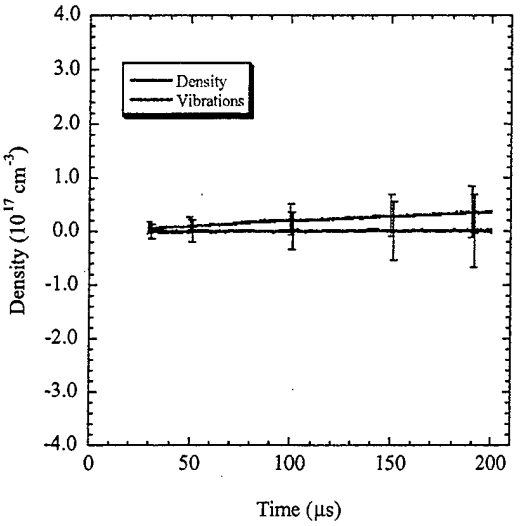


**Figure 5: Neutral density measurements from 13 pass Herriott Cell interferometry. Data taken at 5 mm from fuel face for 6.6 J discharge.**

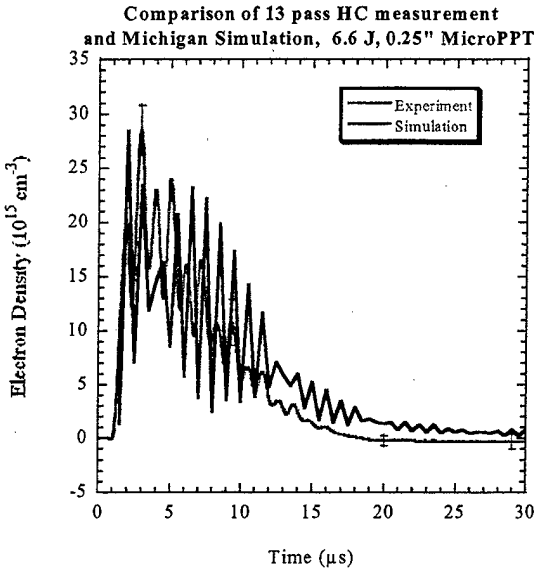


**Figure 6: Comparison of predicted and measured electron density time variation at 5 mm from the propellant face at the axis in the case of 6.35–mm diameter MicroPPT firing at 6.6 J.**

data is taken at 5–mm distance from the fuel face and provides the control case for density measurements with the Herriott Cell.

## Experimental Results and Discussion

*Density Measurements*

The data from the two–color interferometer shows electron and neutral density at 5 mm from the fuel face for 6.6 J discharge and 13 passes. Figure 4 shows this data for the first 30 μs after the discharge. Peak electron density reaches $2.1 \pm 0.3 \times 10^{16}$ cm$^{-3}$.

Over a large number of discharges, uncertainty introduced by vibration effects and shot-to-shot thruster variation overwhelms the neutral density signal disallowing a definitive measurement. For a single discharge, the neutral density is typically resolved. Figure 5 shows neutral density data with typical error bars taken at 5 mm from the fuel face using the 13–pass Herriott Cell. The data indicate that at 200 μs after the discharge, neutral density is no larger than $8.5 \times 10^{16}$ cm$^{-3}$.

*Thruster and Model Comparisons*

A significant finding of this experiment is the degree of agreement between theoretical modeling predictions and experimental results. A basis for comparison is required for some modeling and data performed for systems that are not similar in energy or dimension. The energy–to–area ratio provides such a basis and is used here to investigate the comparison between past and current predictions and measurements.

A hybrid fluid–PIC–DSMC approach is used to predict electron density.[17] The energy–to–area ratio for this model is higher than that of the experimental setup used. This is balanced by increased electron density.

Predictions made for the 6.35–mm diameter MicroPPT show strong agreement with experimental data. Description of the model is given elsewhere.[6,16] Figure 6 shows direct comparison of predicted electron density using an experimental current waveform as input. The red line shows density measured using the Herriott Cell. The degree of agreement is apparent, and provides support for the model being developed.

*External Electron Density*

Herriott cell measurements give strong evidence of plasma presence as much as 3 mm behind the exit plane. A MicroPPT ablation model presented elsewhere predicts non–zero carbon ion densities at the exit outside a 3.1 mm diameter MicroPPT.[17]

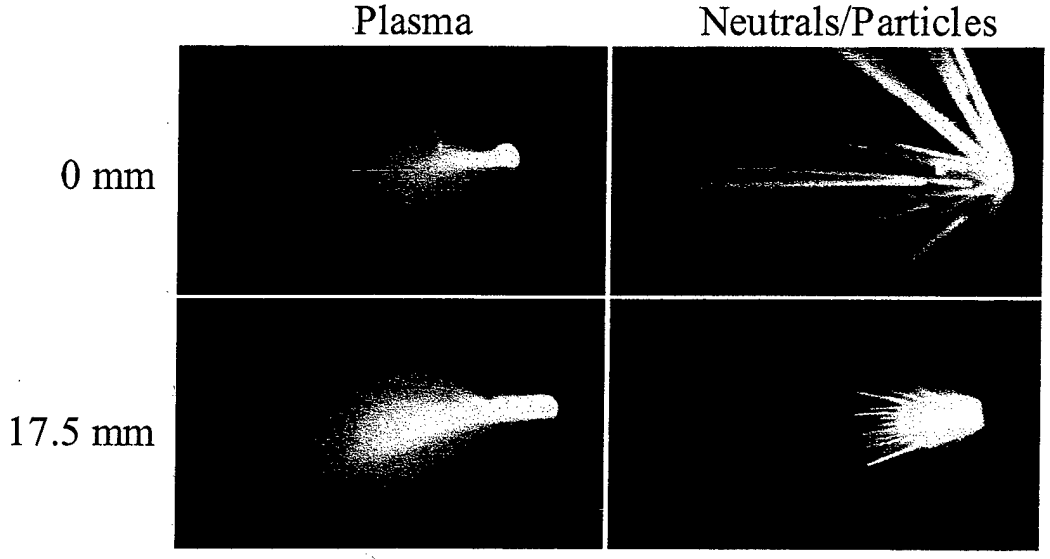


**Figure 7: Plasma and Late Time Vaporization divergence in a ¼"–diameter, 2–electrode MicroPPT firing at 5 J. The curved rod visible in the plasma pictures is a spark plug used to ignite the main discharge**

Plasma backflow and external arc attachment can explain this phenomenon.

*Plume Diagnostics*

In order to better understand the potential for spacecraft integration, further validate the plume model, and help the designers determine the optimal MicroPPT placement on the spacecraft, a series of tests were conducted to characterize the MicroPPT plume divergence. The goal of the test was to characterize the plume divergence for both the initial plasma exhaust and for the late time vaporization (LTV). The LTV consists of neutrals and particles emitted from PPTs for a few milliseconds after the current discharge and plasma has extinguished.[18] Estimates indicate that LTV contains as much as 90% of the expended propellant mass so it is critical to consider this component of the exhaust when considering spacecraft interaction. Plume divergence measurements are collected for the MicroPPT at beginning–of–life (BOL) when the propellant face is at the exit plane of the thruster, and after significant recession has occurred.

The intensity, general shape and size of the observed MicroPPT plume is uniform and repeatable at all propellant depths. LTV images, by their very nature, are erratic from shot–to–shot as they capture trails of individual particles exiting from the thruster rather than a uniform, expanding plasma. Despite this irreproducibility, the overall divergence of the LTV was repeatable at all depths. Figure 7 shows the MicroPPT plume at BOL, and at a fuel depth of 17.5 mm. The plasma plume is initially well–directed with virtually no divergence, a characteristic common at all depths. Further into the flow field, the plasma diffuses into a 60°–70° cone. The increased brightness of the plume at 17.5 mm is not an indication of increased emission; rather the gain of the camera was raised to better resolve the plume shape. At BOL, the MicroPPT is seen to emit particulates into the entire 180° plane at the thruster tip. As the propellant face is recessed into the outer electrode, a dramatic decrease in the LTA divergence angle is observed. The measured divergence angle, as a function of the recession depth of the propellant is shown in Figure 8 for both the plasma and LTV (neutrals/particles) emission. The images of Figure 7 and the plot of Figure 8 suggest that intentionally recessing the propellant face at beginning of life may significantly reduce the potential for spacecraft contamination from the neutrals and particles.

**Recent Diagnostic Efforts**

*Pockels Cell Voltage Measurements*

The MicroPPT poses a unique dilemma for common voltage measurement techniques. Due to the high impedance present in the MicroPPT circuit, conventional high-voltage diagnostics are intrusive and cannot be used. In response to this need,

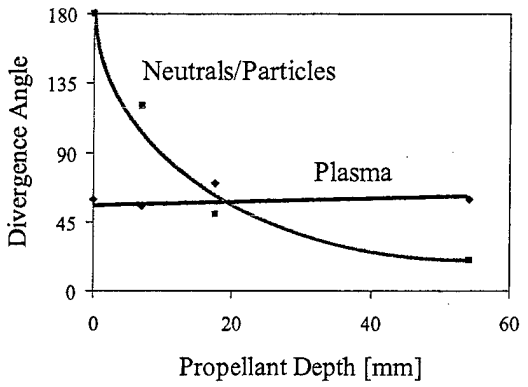


**Figure 8: The divergences of the plasma and LTV effluents. The area affected by potentially contaminating particulates greatly reduces as propellant recesses.**

development of a Pockels Cell voltage measurement is ongoing at AFRL.

A Pockels Cell rotates light polarization in proportion to an applied electric field. A polarized laser is directed through the Cell, rotating the beam polarization as shown in Figure 9. A polarized filter attenuates the beam and the intensity is measured by photodiodes before and after the Pockels Cell and filter combination. The ratio of the beam intensities is a precise and repeatable function of the applied voltage. Since the Pockels Cell draws no current, the infinite impedance assures a non-intrusive measurement of capacitor voltage for the MicroPPT.

*Surface Temperature Measurements*

A model of the plasma layer near the evaporating surface of a MicroPPT has been developed and is described in detail elsewhere.[13] The model includes Teflon™ ablation, plasma energy balance, heat transfer from the plasma to the Teflon™, current spreading in the near field, and an equivalent RLC electrical circuit model. The inputs for the model are thruster geometry, Teflon™ material properties, and Teflon™ equilibrium pressure dependence on the surface temperature.

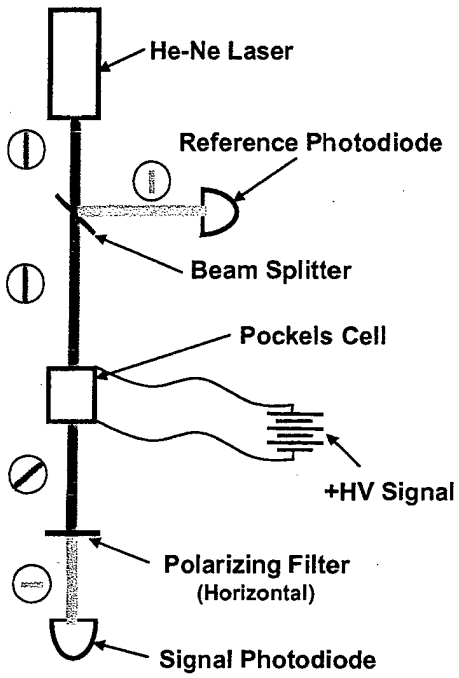


**Figure 9: Pockels Cell voltage measurement schematic**

According to the energy balance and the heat transfer equation at the Teflon™ surface, the surface temperature should depend on the current density. The predicted spatial and temporal variation of the Teflon™ surface temperature is shown in Figure 10. In these calculations, the experimental current waveform is used. Clearly, the Teflon™ surface temperature is radially non-uniform. In the case of the 3.6-mm diameter thruster, the temperature has a minimum at radial distances of 1.1-1.3 mm.

An attempt to experimentally validate the surface temperature predictions is currently underway at AFRL. Infrared emission measurements from the Teflon surface are being explored using techniques common in dynamic crack propagation problems in fracture mechanics. The technique consists of an LN2–cooled Mercury Cadmium Tellurium (HgCdTe) photodetector array with corresponding optics and circuitry. Response time for these arrays varies from 2 – 200 MHz depending on the active area and circuitry.

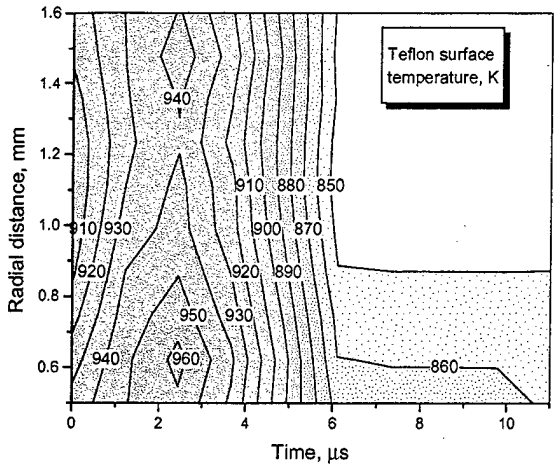


**Figure 10: Temporal and radial distribution of the Teflon™ surface temperature (K) for a 3.6-mm diameter MicroPPT**

This experiment is being designed to provide a spatially– and temporally– resolved surface temperature map throughout the discharge. Of special interest is the temperature decay time after the discharge as an indicator of late-time vaporization. Validation of the model predictions by Keidar and Boyd is a driving factor in this research.

## Conclusions

An examination of the plume of a MicroPPT utilizing a dual–wavelength and a 13–pass Herriott Cell system indicates a peak electron density $n_e = 2.1 \pm 0.3 \times 10^{16}$ $cm^{-3}$. Attempts to measure neutral density with the increased resolution of the interferometer were unsuccessful. For standard PPTs, the Herriott Cell has been effective in measuring neutrals as late as 200 μs after the pulse for single shots, with averaged neutral density measured out to 150 μs.[7] However, previous measurements used the Herriott Cell without external focusing optics and were therefore less susceptible to mechanical vibrations late in time. Past measurements also used higher numbers of passes in the Herriott Cell that are not achieved here. The neutral density is bracketed by an upper limit $n_n = 8.5 \times 10^{16}$ $cm^{-3}$ at 200 μs after the pulse is established.

Agreement between present electron density measurements and numerical predictions is strong. Comparison by the energy–to–area ratio argument for the 3.1–mm MicroPPT matches well using curve–fit data taken here. Also, specific predictions using the current waveform as an input followed measured electron densities very closely. This indicates some level of validation for the numerical model.

Spacecraft interaction tests indicate that the plasma plume shape can be well–characterized and accounted for in spacecraft integration. The divergence of the late time vaporization, which evolves after the plasma, is strongly linked to the recession of the Teflon™ in the MicroPPT. An initial recessing of the fuel at BOL may be necessary to reduce solid Teflon™ deposition on spacecraft surfaces

A Pockels Cell has been developed and is in use as an alternative voltage diagnostic for MicroPPTs. This has been shown to allow voltage measurements in cases where the typical voltmeter impedance is too large to produce a reliable measurement.

A model of the plasma layer near the Teflon™ surface of a MicroPPT was developed that allows a self-consistent calculation of the Teflon™ surface temperature and ablation rate. It is predicted that the Teflon™ surface temperature is non-uniform in the radial direction. To verify these predictions, research on a surface temperature measurement by fast response HgCdTe photodetectors is underway.

## References


[1] M.L. McGuire and R.M. Myers, "Pulsed Plasma Thrusters for Small Spacecraft Attitude Control," GSFC Flight Mechanics/Estimation Theory Symposium, May 13-16, 1996.

[2] R.J. Vondra, "The MIT Lincoln Laboratory Pulsed Plasma Thruster," AIAA Paper No. 76-998, Nov. 1976.

[3] G.G. Spanjers, D.R. Bromaghim, D. White, J. Schilling, S. Bushman, J. Lake, M. Dulligan, "AFRL MicroPPT Development for the TechSat21 Flight," 27th Int'l Electric Propulsion Conference, IEPC paper 2001–166, Pasadena, CA 2001.

[4] G.G. Spanjers and R.A. Spores, "PPT Research at AFRL: Material Probes to Measure the Magnetic Field Distribution in a Pulsed Plasma Thruster," 34th AIAA Joint Propulsion Conf, paper AIAA-98-3659, Cleveland, OH, July 12-15, 1998.

[5] G. G. Spanjers, K. A. McFall, F. S. Gulczinski, R. A. Spores, "Investigation of Propellant Inefficiencies in a Pulsed Plasma Thruster," AIAA Paper No. 96-2723, July 1996.

[6] D.R. Herriott, H. Kogelnik, R. Komfner, "Off Axis Paths in Spherical Mirror Interferometers," Applied Optics, 3, 1964, 523.

[7] E.L. Antonsen, R.L. Burton, S.F. Engelman, G.G. Spanjers, "Herriott Cell Interferometry for Unsteady Density Measurements in Small Scale Length Thruster Plasmas," AIAA Paper No. 2000–3431, July 2000.

[8] E.L. Antonsen, R.L. Burton, G.G. Spanjers, "High Resolution Laser Diagnostics in Millimeter-Scale Micro Pulsed Plasma Thrusters," 27th Int'l Electric Propulsion Conference, IEPC paper 2001–157, Pasadena, CA 2001.

[9] M. Keidar and I.D. Boyd, "Electromagnetic effects in the near field plume exhaust of a pulsed plasma thruster", AIAA Paper 2001-3638, July 2001.

[10] I. D. Boyd, M. Keidar, and W. McKeon, "Modeling of a pulsed plasma thruster from plasma generation to plume far field", Journal of Spacecraft and Rockets, Vol. 37, No. 3, 2000, pp. 399-407

[11] M. Keidar and I.D. Boyd, "Device and plume model of an electrothermal pulsed plasma thruster", Paper AIAA-2000-3430, July 2000.

[12] M. Keidar, J. Fan, I.D. Boyd and I.I. Beilis, "Vaporization of heated materials into discharge plasmas", Journal of Applied Physics, 89, 2001, pp. 3095-3098.

[13] M. Keidar, I.D.Boyd, F.S. Gulczinski III, E.L. Antonsen, G.G. Spanjers, "Analyses of Teflon surface charring and near field plume of a Micro-Pulsed Plasma Thruster," 27th Intl Electric Propulsion Conference, IEPC Paper 2001-155, Pasadena, CA 2001.

[14] G. G. Spanjers, J. H. Schilling, and D. White, "Methods to Increase Propellant Throughput in a Micro Pulsed Plasma Thruster," US Provisional Patent filed July 2001.

[15] E.L. Antonsen, Herriott Cell Interferometry for Pulsed Plasma Density Measurements, MS Thesis, University of Illinois at Urbana-Champaign, 2001.

[16] G. G. Spanjers, K. A. McFall, F. S. Gulczinski, R. A. Spores, "Investigation of Propellant Inefficiencies in a Pulsed Plasma Thruster," AIAA Paper No. 96-2723, July 1996.

[17] M. Keidar, I.D. Boyd, "Electromagnetic Effects in the Near Field Plume Exhaust of a Pulsed Plasma Thruster," AIAA Paper No. 2001-3638.

[18] G. G. Spanjers, J. A. Lotspeich, K. A. McFall, R. A. Spores, "Propellant inefficiency resulting from particulate emission in a Pulsed Plasma Thruster," Journal of Propulsion and Power, Vol. 14, No. 3, May–June 1998.